

# UC Davis

## UC Davis Previously Published Works

### Title

Detection of Acrylamide in Foodstuffs by Nanobody-Based Immunoassays

### Permalink

<https://escholarship.org/uc/item/4xw7g8s5>

### Journal

Journal of Agricultural and Food Chemistry, 70(29)

### ISSN

0021-8561

### Authors

Liang, Yifan

Zeng, Yuyao

Luo, Lin

et al.

### Publication Date

2022-07-27

### DOI

10.1021/acs.jafc.2c01872

Peer reviewed



Published in final edited form as:

*J Agric Food Chem.* 2022 July 27; 70(29): 9179–9186. doi:10.1021/acs.jafc.2c01872.

## Detection of Acrylamide in Foodstuffs by Nanobody-Based Immunoassays

Yifan Liang<sup>1,†</sup>, Yuyao Zeng<sup>1,†</sup>, Lin Luo<sup>1</sup>, Zhenlin Xu<sup>1,2</sup>, Yudong Shen<sup>1</sup>, Hong Wang<sup>1,2,\*</sup>, Bruce D Hammock<sup>3</sup>

<sup>1</sup>Guangdong Provincial Key Laboratory of Food Quality and Safety, College of Food Science, South China Agricultural University, Guangzhou 510642, China.

<sup>2</sup>Guangdong Laboratory for Lingnan Modern Agriculture, Guangzhou 510642, China.

<sup>3</sup>Department of Entomology and Nematology, UCD Comprehensive Cancer Center, University of California, Davis, California 95616, USA.

### Abstract

Acrylamide is toxicant aliphatic amide formed via the Maillard reaction between asparagines and reducing sugars during food heat processing. Herein, a specific nanobody termed Nb-7E against acrylamide derivative xanthyl acrylamide (XAA) was isolated from an immunized phage displayed library and confirmed to be able to detect acrylamide. Firstly, an ic-ELISA was established for acrylamide with the limit of detection (LOD) of 0.089  $\mu\text{g/mL}$  and working range from 0.23  $\mu\text{g/mL}$  to 5.6  $\mu\text{g/mL}$ . Furthermore, an enhanced electrochemical immunoassay (ECIA) was developed based on the optimized reaction conditions. The LOD was low to 0.033  $\mu\text{g/mL}$ , 3-fold improved than that of ic-ELISA and a wider linear detection range from 0.39  $\mu\text{g/mL}$  to 50.0  $\mu\text{g/mL}$  was achieved. The average recoveries ranged from 88.29% to 111.76% in spiked baked biscuits and potato crisps. Finally, the analytical performance of ECIA was validated by the standard ultra-performance liquid chromatography-tandem mass spectrometry (UPLC-MS/MS).

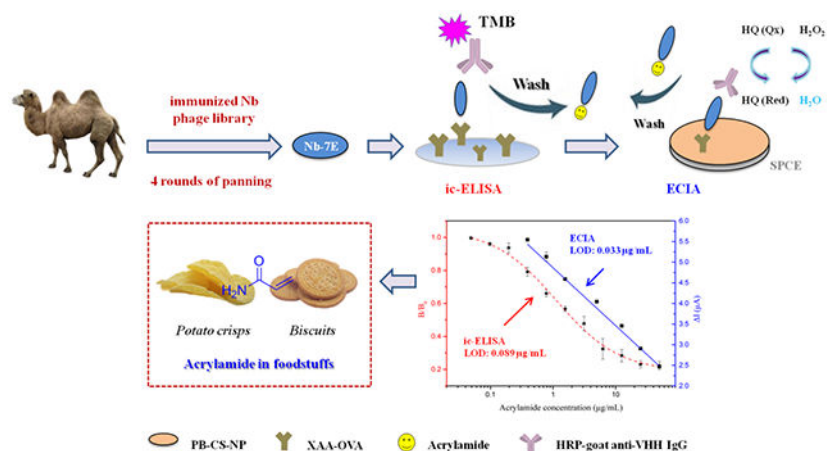
### Graphical Abstract

\*Corresponding author: Hong Wang, gzwhongd@163.com; Tel: +86-20-85283448; Fax: +86-20-85280270.

<sup>†</sup>Equal contribution.

The authors declare no competing financial interest.

All procedures involving animals were performed in accordance with the relevant protective and administrative guidelines for laboratory animals of China.



## Keywords

acrylamide; nanobody; ELISA; electrochemical immunoassay

## Introduction

Acrylamide (AA, Mw 71.08 Da) is a vinylic hazardous chemical, which has inherently toxic properties, including neurotoxicity, reproductive toxicity, and carcinogenicity<sup>1</sup>. Therefore, it was listed by the International Agency for Research on Cancer as a probable human carcinogen in group 2A<sup>2</sup>. Since it was found and firstly reported in fired or oven-cooked carbohydrate-rich foods in 2002<sup>3-4</sup>, food-borne AA contamination has been getting more and more public concern. The survey by Konings et al. showed that the mean amounts of AA in the cocktail snacks were the highest among the detected food samples and up to 1060 µg/kg, then gingerbread with 890 µg/kg and chips with 351 µg/kg<sup>5</sup>. In 2015, European Food Safety Authority (EFSA) regulated that the amount of AA in potato crisps should be below the indicative value of 1000 µg/kg<sup>6</sup>. However, the reference level for AA in potato crisps was monitored as 750 µg/kg by the European Union (EU)<sup>7</sup>. Therefore, given its toxicity and high pollution levels, a rapid, portable and highly sensitive detection method for AA would be helpful in monitoring the safety of foodstuffs more conveniently and making dietary exposure assessment with more extensive coverage.

So far, some methods have been used to quantify AA in foodstuffs. Most of them suffer significantly from high instruments cost and complex operations, such as high-performance liquid chromatography (HPLC), gas chromatography (GC) and capillary electrophoresis (CE) separations<sup>8-10</sup>. Alternatively, immunoassays based on the specificity of antibodies to recognize target antigens are paid more attention for their excellent sensitivity, high-throughput screening and ease of combination with other detection formats, especially in detection of small molecule compounds in foodstuffs. Till now, several immunoassays have been reported for AA<sup>11-13</sup>. For example, Zhu et al. prepared a monoclonal antibody (mAb) against the derivative of AA (4-mercaptophenylacetic acid derivatized AA, AA-4-MPA) and developed an indirect competitive enzyme-linked immunosorbent assay (ic-ELISA) for AA determination<sup>14</sup>. Furthermore, an electrochemical immunosensor was established with a

polyclonal antibody (pAb) specific for AA-4-MPA as recognition element, achieving a 100-fold improvement in sensitivity and decreasing analysis time in comparison to the original ic-ELISA<sup>15</sup>. Meanwhile, using 9-xanthidrol as derivative, Luo et al. also prepared the specific antibodies for 9-xanthidrol derivatized AA (XAA) and developed the fluorescence immunoassay for AA with the limit of detection low to 0.16 ng/mL<sup>16</sup>. However, the traditional antibodies have limitations including the unstable quality of pAbs caused by the batch-to-batch variation of immunized animals or the specificity loss of mAbs during thawing of hybridoma when it expressed additional functional variable regions<sup>17</sup>. So, a novel type of antibody with more excellent characteristics would be urgently demanded.

Nanobodies (Nbs), termed variable heavy chain (VHH) domains, are derived from the heavy-chain-only antibody in Camelidae<sup>18</sup>. Compared with traditional pAbs or mAbs, Nbs have unique physiochemical advantages in terms of high robustness to harsh conditions, ease of production by prokaryotic expression system<sup>19–20</sup>. Due to its small size, Nb binds to a higher density on the surface of immunosensors, which can increase the signal-to-noise ratio, resulting in the enhanced sensitivity. For instance, Liu et al. described a nanobody-based ECIA for ultra-sensitive detection of AFB1, allowing two orders of magnitude improvement in LOD over mAb-based ECIA<sup>21</sup>. This suggests that Nbs might circumvent problems encountered with classical antibodies to detect small molecule contaminants, thus creating a novel detection system.

In this study, a phage displayed library derived from an immunized Bactrian camel was constructed with the designed XAA-BSA as immunogen, then the specific Nbs were screened out and the characteristics were confirmed. Meanwhile, an ic-ELISA was established for AA detection based on the optimal Nb. To further improve the assay performance, an electrochemical immunoassay was developed under the optimized reaction conditions for detecting AA in potato crisps and biscuits samples (Scheme 1). Finally, the method was validated by the standard UPLC-MS/MS.

## Experimental methods

### Materials and reagents

Acrylamide was supplied by Aladdin Chemical Technology Co., Ltd (Shanghai, China). Complete and incomplete Freund's adjuvants, bovine serum albumin (BSA), ovalbumin (OVA) and keyhole limpet hemocyanin (KLH) were purchased from Sigma Aldrich (St. Louis, MO, USA). Xanthyl acrylamide derivatives (XAA), xanthyl methyl carbamate (XMC) and xanthyl ethyl carbamate (XEC)<sup>16</sup>, XAA-BSA as immunogen and XAA-OVA as coating antigen, and anti-XAA mAb were prepared previously in our lab<sup>22</sup>. The total RNA extraction kit was from Guangzhou Gbcbio Technologies Inc. (Guangzhou, China). The first strand cDNA synthesis kit was purchased from Takara (Dalian, China). The gel extraction and PCR purification kit were from Tiangen Biotech Co., Ltd. (Beijing, China). Helper phage M13KO7, restriction enzyme, T4 DNA ligase and others, were obtained from New England Biolabs (MA, USA). 9-xanthidrol, other organic solvents and chemicals were of analytical grade from Sigma (St. Louis, USA) and Thermo Fisher Scientific (Thermo, USA).

### Construction and identification of phage displayed nanobody library

A three-year-old male Bactrian camel was immunized subcutaneously with 500 µg of XAA-BSA and Freund's adjuvant mixture biweekly. The nanobody phage displayed library was constructed by using the method described previously<sup>18, 23</sup>. Briefly, after sixth immunization, fresh blood was collected and used for lymphocyte isolation, followed by RNA extraction, cDNA synthesis and VHH gene amplification by two-nested PCR. The purified PCR product was ligated into pComb3xss phagemid vector digested by restriction enzyme *Sfi*I and then transformed into *E.coli* TG1 competent cells. All cells plated on LBA agar (10 g/L tryptone, 5 g/L yeast extract, 10 g/L NaCl, supplemented with 100 µg/L ampicillin and 15 g/L agar) were collected and rescued by helper phage M13KO7 to prepare an immunized VHH phage displayed library. The capacity and diversity were evaluated by sequence analysis of randomly 10 clones.

### Selection and characterization of nanobody against XAA

The procedure of phage biopanning was performed as described before with some modifications<sup>23</sup>. Namely, three wells of microplate were coated overnight with 100 µL of XAA-OVA (10 µg/mL) in PBS (0.01 M), and additional one well with 100 µL of mixture of 2% KLH, OVA and BSA solution. After washing 5 times with PBST (PBS with 0.1% Tween-20), all wells were blocked with 1% fish gelatin at 37 °C for 2 h. Then, 100 µL/well of nanobody phage library was added into well coated with mixture of KLH, OVA and BSA at 37 °C for 1 h. The unbound phages were dispensed into three antigen-coated wells (100 µL/well). After incubating for 1 h, the three wells were washed 5 times with 0.1% PBST and 15 times with PBS respectively. The bound phages were eluted with 100 µL/well of 0.2 M Gly-HCl solution (pH 2.2) at 37 °C for 10 min and then immediately neutralized with 12 µL/well of 1 M Tris-HCl (pH 9.1). The eluent (10 µL) in each round were diluted to determine the output titer, and other was amplified for the next round of biopanning. In the following second, third and fourth round, competitive elution method was carried out with different concentration of XAA (1000, 500 and 100 ng/mL). The concentration of XAA-OVA was decreased to 2, 0.4, 0.08 µg/mL, and the content of Tween-20 in PBST increased from 0.2 to 0.3, and 0.4% respectively. To decrease the nonspecific binding, three kinds of blocking buffers including 3% skimmed milk, 1% fish gelatin and 3% skimmed milk were utilized. After the fourth-round panning was finished, several clones were randomly picked up from the output plates to test their binding ability with XAA by ic-ELISA<sup>23</sup>. The positive clones were sequenced for further analysis.

### Expression, purification and identification of anti-XAA Nbs

The vector pComb3xss-Nb was transformed into competent cells *E.coli* BL21 (DE3). After sequencing confirmation, individual clone was selected and cultivated in LBA medium (10 g/L tryptone, 5 g/L yeast extract, 10 g/L NaCl, supplemented with 100 µg/L ampicillin) with shaking at 250 rpm overnight. A 6 mL-aliquot of overnight culture was inoculated to 600 mL of LBA medium and shaken at 37 °C until OD<sub>600</sub> value reached around 0.6, followed by the addition of 1 mM of isopropyl β-D-thiogalactopyranoside (IPTG) for production of nanobody. The supernatant was collected by Sorvall Lynx 4000 centrifuges (Thermo Fisher Scientific, USA), and then purified on a 1-mL Ni-NTA resin column. The purified Nb was

dialyzed in PBS buffer and identified by SDS-PAGE and western blotting according to the standard protocols<sup>24</sup>, and the concentration was determined by using NanoDrop 2000C system (Thermo Fisher Scientific, USA).

### Procedure of Nb-based ic-ELISA

The ic-ELISA protocol was performed as described before with minor modifications<sup>23</sup>. As shown in more detail below, 100  $\mu\text{L}$  per well of XAA-OVA in PBS was used to coat a 96-well microplate overnight at 37  $^{\circ}\text{C}$ . The plate was washed twice with PBST (0.01 M PBS containing 0.05% Tween-20) and then blocked with 2% skimmed milk in PBS at 37  $^{\circ}\text{C}$  for 2 h. After discarding the blocking solution, the plate was dried at 37  $^{\circ}\text{C}$  for 30 min and stored at 4  $^{\circ}\text{C}$  until use. A serial of AA standards with different concentrations (0–50  $\mu\text{g}/\text{mL}$  in PBS) were prepared via the following derivatization reaction. First, AA standard (0.6 mL) was mixed with 0.4 mL of 9-xanthidrol (4 mg/mL), then 0.1 mL of HCl (0.5 M) was added to trigger the reaction. After 30 min, the reaction was finished by adding 0.1 mL of NaOH (0.5 M). The mixture solution was used as competitor. Each well was added with 50  $\mu\text{L}$  of competitor and 50  $\mu\text{L}$  of Nb solution at optimal concentration. After incubated at 37  $^{\circ}\text{C}$  for 30 min and washed five times with PBST, the diluted HRP-goat anti-VHH IgG (Abcam, Guangzhou) was added to the wells with 30 min incubation at 37  $^{\circ}\text{C}$ , followed by a washing step with PBST (five times). Finally, 100  $\mu\text{L}/\text{well}$  of TMBZ solution was added and the color was stopped after 10 min incubation by addition of 50  $\mu\text{L}$  of 10%  $\text{H}_2\text{SO}_4$ . The absorbance value at 450 nm was measured using a Multiskan MK3 microplate reader (Thermo LabSystems, USA). Furthermore, the standard curve was obtained with a four-parameter fitting module of Origin 9.0. The limit of detection (LOD) was determined as AA concentration at 10% of maximum value calculated from standard curve, and the detectable concentration range was defined as the AA concentration that inhibited 20–80% of maximum value. The rate of cross reactivity was calculated as follows<sup>23</sup>:  $\text{CR} (\%) = \text{IC}_{50} (\text{XAA}, \mu\text{g}/\text{mL}) / \text{IC}_{50} (\text{cross-reactant}, \mu\text{g}/\text{mL})$ .

### Construction and development of nanobody-based ECIA for AA

Prior to modification, a portable commercial screen-printed carbon electrode (SPCE, Zensor R&D, Taiwan) was electrochemically activated by performing a 15-segment cyclic voltammetry scan in 0.2 M  $\text{KNO}_3$  with a potential range from  $-0.1$  to  $+0.1$  V at a scan rate of 50 mV/s, and then the electrode was washed with ultrapure water and dried. Prussian blue-chitosan-nanoparticle (PB-CS-NP) film was electrodeposited on SPCE electrode in a fresh solution including 2.5 mM  $\text{FeCl}_3$ , 2.5 mM  $\text{K}_3[\text{Fe}(\text{CN})_6]$ , 1 mM KCl, 1 mM HCl and 0.05% chitosan with potential range of  $-1$  to  $+1$  at a scan rate of 50 mV/s. After rinsed with ultrapure water and dried, 5  $\mu\text{L}$  of XAA-OVA was dispersed on the working surface of the PB-CS-NP/SPCE and incubated at 4  $^{\circ}\text{C}$  overnight, and the unbound was removed by washing with 0.01 M PBS. Subsequently, 5% skimmed milk (5  $\mu\text{L}$ ) was coated on the electrode surface at 37  $^{\circ}\text{C}$  for 1 h. Finally, the immunosensor was washed thoroughly with 0.01 M PBS and stored at 4  $^{\circ}\text{C}$  until used. The diluted Nb solution together mixed with different concentration of competitor was spotted onto the modified SPCE surface at 37  $^{\circ}\text{C}$  for 30 min. After the washing steps, 5  $\mu\text{L}$  of HRP-goat anti-VHH IgG was added for another 30 min reaction. As for electrochemical detection, the modified immunosensor was immersed in 0.01 M PBS containing 1 mM HQ and 6%  $\text{H}_2\text{O}_2$  and performed on a CHI660D

electrochemical work station (CH Instruments, Shanghai Chenhua Instrument Corporation, Shanghai, China). The change in the electrochemical cathodic current before and after the addition of H<sub>2</sub>O<sub>2</sub> was used as the signal response (I), and then we could obtain the standard curve between the concentrations of AA and I value. Consequently, the limit of detection (LOD) was defined as the equation:  $LOD = Y + 3SD$ , where Y is the mean signal of the blank measurements, and SD is the standard deviation of blank measurements, and a value of 3 refers to the equation constant. The lower and upper limits of quantitative concentration were defined as linear range<sup>25</sup>.

### Analysis of spiked samples based on ECIA

Biscuits and potato crisps samples were purchased from a local supermarket. The samples were first analyzed to obtain the background level of AA and then used to perform the recovery test. Briefly, 10 g of sample spiked with different concentration of AA was mixed with 40 mL of methanol and homogenized, followed by the defatting step using 5 mL of n-hexane and centrifugation at 4500 rpm for 10 min. The supernatants were evaporated to dryness and dissolved in 5 mL of distill water. The following derivatization as above described and the mixture solution was used for further analysis.

### Assay validation by UPLC-MS/MS

The nanobody-based ECIA was validated by UPLC-MS/MS operated at the Guangzhou Institute for Food Control, China. The conditions were as follows: the C18 column (150 mm × 4.6 mm, 5 μm) was used for chromatographic separation at 40 °C. The mobile phases were 0.3% acetic acid and acetonitrile at the ratio of 95: 5 (v/v). The flow rate was 0.5 mL/min, and the injection volume of each sample was 20 μL. An AB TRIPLE QUAD 4500 Mass Spectrometer (AB, USA) was operated in ESI mode set as positive ionization multiple reactions monitoring (MRM) scanning mode. Other ionization source parameters were also optimized and set as follows: source cone temperature: 450 °C, drying gas flow: 6 L/min, detection voltage: 5.5 kV, nebulizer gas: 40 psi. The parent and daughter ion of AA were m/z 72 as well as m/z 55 and 44, respectively.

## Results and discussion

### Library construction, biopanning and expression

For the molecular weight of AA is too low, until now, the immunoassays for AA mostly utilized the antibodies specific for its different derivatives<sup>12–13</sup>. In the previous study of our group, 9-xanthinol was demonstrated to be efficient to convert AA into XAA with simple procedures and the prepared anti-XAA pAb showed the high affinity to XAA<sup>16</sup>. Therefore, XAA-BSA (Figure S1) was still used as immunogen in this work. After the sixth immunization to the Bactrian camel, the inhibition rate of the serum for XAA was more than 85%, so the peripheral blood lymphocyte was collected and cDNA was extracted then to construct the phage displayed library with the reported methods as reference<sup>18, 23</sup>. Considering that an immunized antibody library might possess higher possibility to contain the target Nbs, the constructed library with a little low capacity of  $1.0 \times 10^5$  cfu/mL was still used to select the target Nbs. Actually, after four rounds of panning, 10 positive clones were obtained and exhibited binding activity to coating antigen with the inhibition rates for



XAA ranged from 46.00% to 77.53% (Figure 1A). By the sequence alignments analysis, all Nbs clones have the same length but are slightly different in framework region 1 (FR1) and framework region 4 (FR4) (Figure 1B). Therefore, they were confirmed as the same group of Nbs and Nb-7E with the highest inhibition rate was chosen for further analysis. After expressed in *E.coli* BL21 (DE3) host strains, the supernatant containing Nb-7E was purified with Ni-NTA affinity columns, and then identified by SDS-PAGE and western blotting. As shown in Figure 1C, the size of Nb-7E was approximately 18 kDa, which is consistent with the theoretical molecular weight of Nb and the yield was about 7.45 mg/L with the purity higher than 90%.

### Stability of anti-XAA Nb-7E

Generally, Nbs possess great thermostability and the tolerance to organic solvent. Herein, the stability of the obtained Nb-7E was confirmed with the anti-XAA mAb as control. It was found that Nb-7E was able to bind to antigen at temperature as high as 95 °C, while mAb lost its activity very quickly after 5 min incubation at 80 °C. Even more, Nb-7E retained about 100% of binding activity after incubation for 1 h at 85 °C, however, mAb could only endure 10 min (Figure 2A–B). Normally, the additional disulfide bonds formed by cysteine (Cys) residues existed in Nbs were thought to contribute to reversibly refold and retain binding activity when encountering heat-induced denaturation<sup>26</sup>. According to the sequence of Nb-7E, four Cys might form two disulfide bonds, resulting in the robustness to harsh conditions.

Meanwhile, methanol and acetonitrile, two kinds of organic solvents commonly used in pretreatment of samples were chosen to test the tolerance of Nb-7E. As shown in Figure 2C, with increase of methanol concentration, both Nb-7E and mAb gradually lost the activities. When the concentration of methanol was up to 70%, Nb-7E could still maintain over 70% of binding activity, whereas mAb lost almost all bioactivity. In the contrary, mAb as a whole had superior performance than did Nb-7E in tolerance for acetonitrile (Figure 2D). It has been reported that some amino acids including Met4, Pro43 and Gly66 of V<sub>L</sub> or Ile2, Leu37, Ile48 and Gly49 of V<sub>H</sub> might improve the antibodies' tolerance to acetonitrile<sup>27</sup>. By alignment sequence analysis, we found the mAb just exactly has Met4, Pro44 and Gly66 in V<sub>L</sub>, Gly49 in V<sub>H</sub> (Table S2) yet Nb-7E contains no these residues at the same sites (Val2/37/48 and Ala49), therefore exhibited poorer resistance to acetonitrile.

### Establishment of ic-ELISA based on Nb-7E

Considering the influence of assay parameters, several factors were optimized to develop an ic-ELISA with Nb-7E for AA. After the checkerboard procedure, 2 µg/mL of XAA-OVA and 3.4 µg/mL of Nb-7E were selected as the optimal concentrations. Other assay parameters including an incubation time of 30 min and a dilution of 1: 2500 of HRP-goat anti-VHH IgG as well as dilution buffer with 0.01 M PBS were determined (Figure S2). Under the optimal reaction conditions, an ic-ELISA was established and the limit of detection (LOD) for AA was 0.089 µg/mL with working range from 0.23 to 5.6 µg/mL (Figure 2E), which could meet the regulation standard by the EU. Compared to the previous reported ic-ELISA based on the other derivative such AA-4-MPA<sup>14</sup>, the established ic-



ELISA in this work was more rapid and simpler because the derivatization by 9-xanthidrol was more gentle under the room temperature (25 °C) with less time (< 30 min).

Additionally, the cross-reactivity (CR) test showed that except for the analog XMC, there was negligible CR to XEC and 9-xanthidrol (Figure 2F). By homology modeling of Nb-7E and docking with XAA or its analogs, it was found that Nb-7E formed a pocket to recognize only XAA and XMC but not XEC or 9-xanthidrol. The interaction forces between Nb-7E and XAA or XMC were both mainly induced by the formed three hydrogen bonds (Figure S3), however, further bonds distance between Nb-7E and XMC might lead to weaker interaction therefore 15.7% of CR.

### Enhanced Nb-7E-based ECIA for AA

To further improve the sensitivity of the assay, the enhanced ECIA based on Nb-7E was developed. Several analytical parameters were confirmed including XAA-OVA concentration, Nb-7E dilution and H<sub>2</sub>O<sub>2</sub> concentration. The higher current response, the higher sensitivity of assay. As shown in Figure 3A, the current response increased gradually with the increment of XAA-OVA concentration, and the maximum response at a concentration of 10 µg/mL was observed. Nevertheless, the higher concentrations of 10 µg/mL prompted a decline in the current. This may be because steric hindrance of the film obstructs the Nb-7E to reach the binding sites and the moving of electrons. Therefore, 10 µg/mL of XAA-OVA was chosen for subsequent study. Similarly, the other optimized conditions included a dilution of 1: 40 of Nb-7E (Figure 3B), and a concentration of 6% H<sub>2</sub>O<sub>2</sub> (Figure 3C). Under the optimum conditions, I values of different concentration of AA were recorded and a linear calibration curve was obtained in the working range from 0.39 to 50 µg/mL represented by  $I (\mu A) = (4.86 \pm 0.01) - (1.4 \pm 0.01) \times \lg C_{AA} (\mu g/mL)$  with a correlation coefficient of 0.99 (Figure 3D–E). The LOD value of the ECIA was 0.033 µg/mL, 3-fold lower than that of ic-ELISA, and a wider linear range was also observed (Table 1). Besides, the ECIA based on Nb-7E has the advantages over that on traditional mAb or pAb in antibodies production, cost and physiochemical stability.

### Analysis of spiked samples by ECIA and UPLC-MS/MS

Biscuits (background level of AA was 289.50 ng/g) and potato crisps (background level of AA was 74.03 ng/g) were analyzed after spiking with different concentration of AA (25, 50, and 75 ng/g). Results showed that average recoveries in spiked samples for ECIA were 88.29% to 111.76% and coefficient of variations (CVs) were all less than 5% (Table 2). The detection results were also validated by UPLC-MS/MS and the correlation coefficient between ECIA and UPLC-MS/MS was up to 0.997 (Figure 4). It means the proposed ECIA based on Nb-7E had a good accuracy for quantitative analysis of AA in foodstuffs.

In this study, specific Nbs against acrylamide derivative xanthyl acrylamide (XAA) were for the first time isolated from a camel immunized nanobody library. Based on the specific Nb-7E, an ic-ELISA for AA was established, furthermore, an enhanced ECIA biosensor with a wider linear range and improved sensitivity was constructed. The LODs of these two methods were far below 750 µg/kg, the regulation standard by the European Union for AA. The accuracy of the proposed ECIA was also testified by the standard UPLC-MS/MS,

which suggested the generation of Nbs in this work can be used as a novel reagent in immunoassays and the established methods were proved to be effective and prospective for AA detection in foodstuffs.

## Supplementary Material

Refer to Web version on PubMed Central for supplementary material.

## Funding

This work was supported by Lingnan Modern Agricultural Science And Technology Guangdong Laboratory Independent Scientific Research Project (NZ2021032), Natural Science Foundation of China (31972157), National Key R&D Program of China (2019YFE0116600), Key-Area Research and Development Program of Guangdong Province (2019B020211002), Guangdong Province Universities and Colleges Pearl River Scholar Funded Scheme (2017), Guangdong Provincial Key Laboratory of Food Quality and Safety (2020B1212060059).

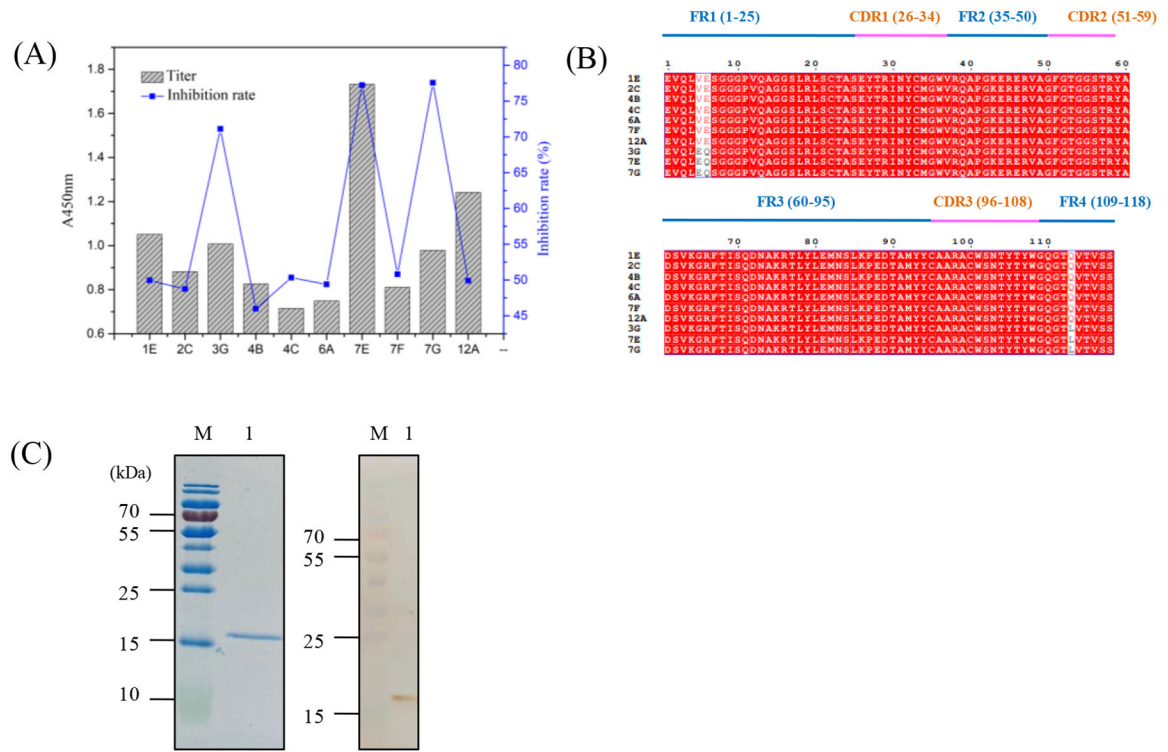
## Supporting information

Synthetic route to complete antigens, parameter optimization of ic-ELISA, docking of Nb-7E and XAA/XMC, primers used to amplify VHH gene and sequence of variable regions of XAA-mAb.

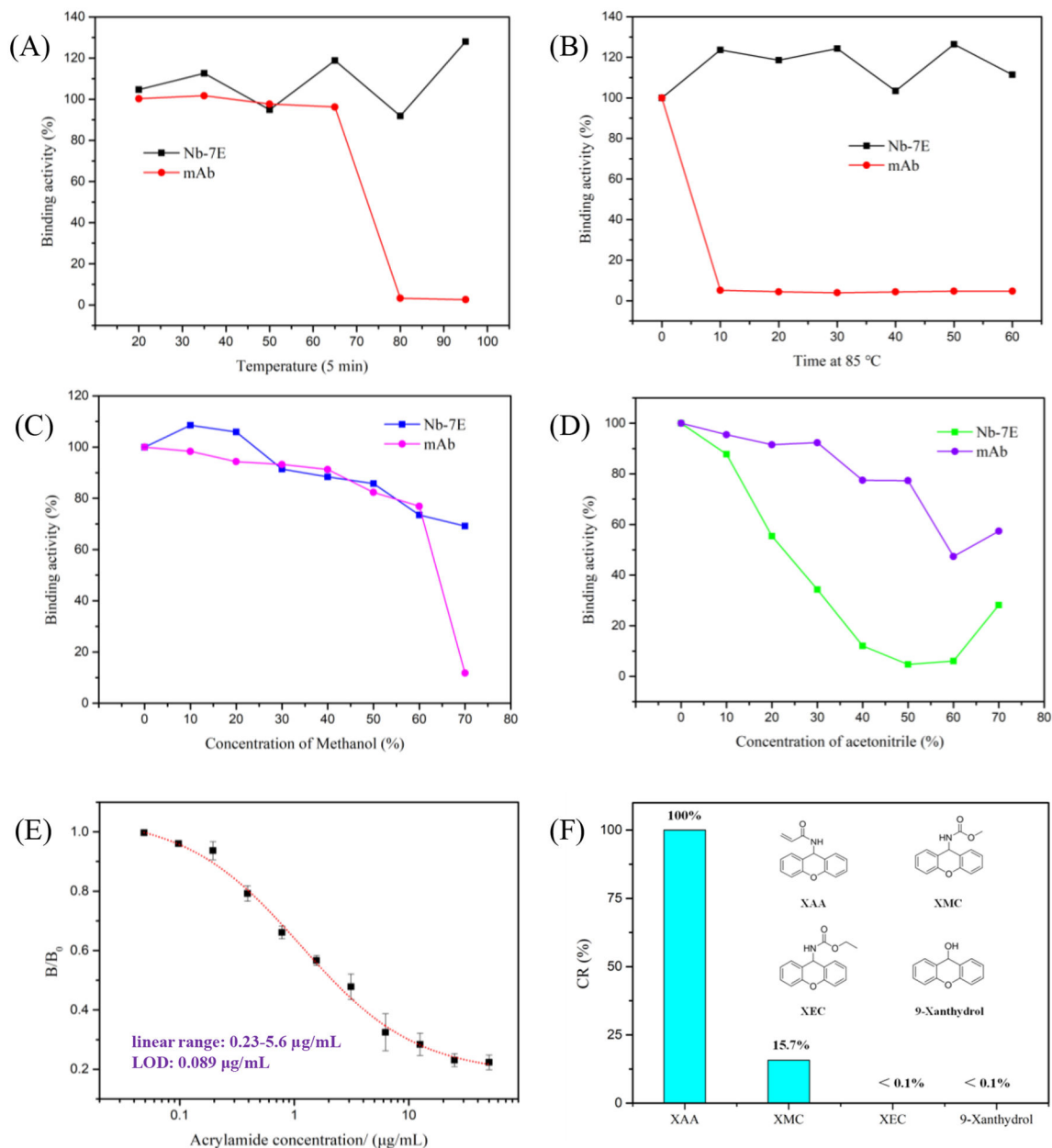
## References

- (1). Zhang Y; Ren YP; Zhang Y New Research Developments on Acrylamide: Analytical Chemistry, Formation Mechanism, and Mitigation Recipes. *Chemical Reviews*. 2009, 109, 4375–4397. [PubMed: 19663380]
- (2). International Agency for Research on Cancer, Lyon, France, 1994, pp 270.
- (3). Authority EFS. Results on acrylamide levels in food from monitoring year 2008. *EFSA Journal*. 2010, 8.
- (4). Svensson K; Abramsson L; Becker W; Glynn A; Hellenas KE; Lind Y; Rosen J Dietary intake of acrylamide in Sweden. *Food and Chemical Toxicology*. 2003, 41, 1581–1586. [PubMed: 12963011]
- (5). Konings EJM; Baars AJ; van Klaveren JD; Spanjer MC; Rensen PM; Hiemstra M; van Kooij JA; Peters PWJ Acrylamide exposure from foods of the Dutch population and an assessment of the consequent risks. *Food and Chemical Toxicology*. 2003, 41, 1569–1579. [PubMed: 12963010]
- (6). EFSA CONTAM Panel. Scientific opinion on acrylamide in food. *EFSA Journal*. 2015, 13, 4104.
- (7). Rayappa MK; Viswanathan PA; Rattu G; Krishna PM Nanomaterials Enabled and Bio/Chemical Analytical Sensors for Acrylamide Detection in Thermally Processed Foods: Advances and Outlook. *Journal of Agricultural and Food Chemistry*. 2021, 69, 4578–4603. [PubMed: 33851531]
- (8). Hoenicke K; Gatermann R; Harder W; Hartig L Analysis of acrylamide in different foodstuffs using liquid chromatography–tandem mass spectrometry and gas chromatography–tandem mass spectrometry. *Analytica Chimica Acta*. 2004, 520, 207–215.
- (9). Zhang Y; Dong Y; Ren YP; Zhang Y Rapid determination of acrylamide contaminant in conventional fried foods by gas chromatography with electron capture detector. *Journal of Chromatography A*. 2004, 1116, 209–216.
- (10). Elisabet B; Oscar N; Luis P; Maria TG Analysis of acrylamide in food products by in-line preconcentration capillary zone electrophoresis. *Journal of Chromatography A*. 2006, 1129, 129–134. [PubMed: 16843477]
- (11). Zhou S; Zhang C; Wang D; Zhao MP Antigen synthetic strategy and immunoassay development for detection of acrylamide in foods. *Analyst*. 2008, 133, 903–909. [PubMed: 18575643]
- (12). Quan Y; Chen ML; Zhan YH; Zhang GH Development of an Enhanced Chemiluminescence ELISA for the Rapid Detection of Acrylamide in Food Products. *Journal of Agricultural and Food Chemistry*. 2011, 59, 6895–6899. [PubMed: 21639145]

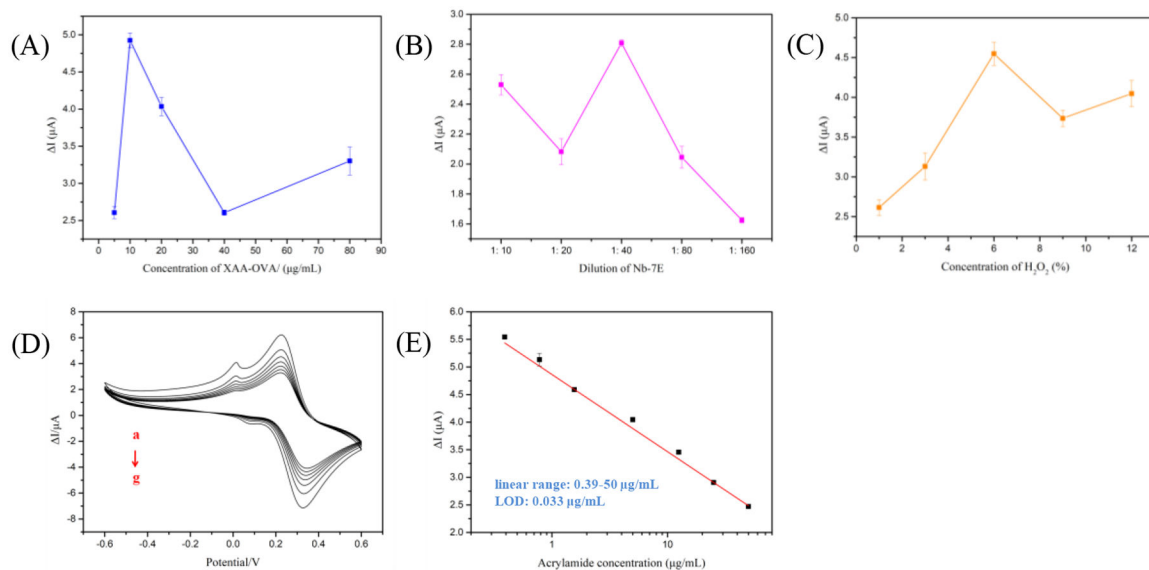
- (13). Wu J; Shen YD; Lei HT; Sun YM; Yang JY; Xiao ZL; Wang H; Xu ZL Hapten Synthesis and Development of a Competitive Indirect Enzyme-Linked Immunosorbent Assay for Acrylamide in Food Samples. *Journal of Agricultural and Food Chemistry*. 2014, 62, 7078–7084. [PubMed: 24998485]
- (14). Zhu YT; Song SS; Liu LQ; Kuang H; Xu CL An indirect competitive enzyme-linked immunosorbent assay for acrylamide detection based on a monoclonal antibody. *Food and Agricultural Immunology*. 2016, 27, 796–805.
- (15). Wu MF; Wang Y; Li S; Dong XX; Yang JY; Shen YD; Wang H; Sun YM; Lei HT; Xu ZL Ultrasensitive immunosensor for acrylamide based on chitosan/SnO<sub>2</sub>-SiC hollow sphere nanochains/gold nanomaterial as signal amplification. *Analytica Chimica Acta*. 2019, 1049, 188–195. [PubMed: 30612650]
- (16). Moraes JZ; Hamaguchi B; Braggion C; Speciale ER; Aguiar RB Hybridoma technology: is it still useful? *Current Research in Immunology*. 2021, 2, 32–40. [PubMed: 35492397]
- (17). Zhang YQ; Xu ZL; Wang F; Cai J; Dong JX; Zhang JR; Si R; Wang CL; Wang Y; Shen YD; Sun YM; Wang H Isolation of Bactrian Camel Single Domain Antibody for Parathion and Development of One-Step dc-FEIA Method Using VHH-Alkaline Phosphatase Fusion Protein. *Analytical Chemistry*. 2018, 90, 12886–12892. [PubMed: 30256086]
- (18). van der Linden RH; Frenken LG; de Geus B; Harmsen MM; Ruuls RC; Stok W; de Ron L; Wilson S; Davis P; Verrips CT Comparison of Physical Chemical Properties of Llama VHH Antibody Fragments and Mouse Monoclonal Antibodies. *Biochimica et Biophysica Acta*. 1999, 1431, 37–46. [PubMed: 10209277]
- (19). Liu Y; Huang H Expression of Single-Domain Antibody in Different Systems. *Applied Microbiology and Biotechnology*. 2018, 102, 539–551. [PubMed: 29177623]
- (20). Liu X; Wen YP; Wang WJ; Zhao ZT; Han Y; Tang KJ; Wang D Nanobody-based electrochemical competitive immunosensor for the detection of AFB1 through AFB1-HCR as signal amplifier. *Microchimica Acta*. 2020, 187, 352. [PubMed: 32462392]
- (21). Luo L; Lei HT; Yang JY; Liu GL; Sun YM; Bai WD; Wang H; Shen YD; Chen S; Xu ZL Development of an indirect ELISA for the determination of ethyl carbamate in Chinese rice wine. *Analytica Chimica Acta*. 2017, 950, 162–169. [PubMed: 27916121]
- (22). Luo L; Jia BZ; Wei XQ; Xiao ZL; Wang H; Sun YM; Shen YD; Lei HT; Xu ZL Development of an inner filter effect-based fluorescence immunoassay for the detection of acrylamide using 9-xanthidrol derivatization. *Sensors and Actuators B: Chemical*. 2021, 332, 129561.
- (23). Wang F; Li ZF; Yang YY; Wan DB; Vasylieva N; Zhang YQ; Cai J; Wang H; Shen YD; Xu ZL; Hammock BD Chemiluminescent Enzyme Immunoassay and Bioluminescent Enzyme Immunoassay for Tenuazonic Acid Mycotoxin by Exploitation of Nanobody and Nanobody-Nanoluciferase Fusion. *Analytical Chemistry*. 2020, 92, 11935–11942. [PubMed: 32702970]
- (24). Liang YF; Wang Y; Wang F; Li JD; Wang CL; Dong JH; Ueda H; Xiao ZL; Shen YD; Xu ZL; Wang H An enhanced open sandwich immunoassay by molecular evolution for noncompetitive detection of *Alternaria* mycotoxin tenuazonic acid. *Food Chemistry*. 2021, 361, 130103. [PubMed: 34082388]
- (25). Dong XX; Yang JY; Luo L; Zhang YF; Mao CB; Sun YM; Lei HT; Shen YD; Beier RC; Xu ZL Portable amperometric immunosensor for histamine detection using Prussian blue-chitosan-gold nanoparticle nanocomposite films. *Biosensors and Bioelectronics*. 2017, 98, 305–309. [PubMed: 28697442]
- (26). Kunz P; Zinner K; Mücke N; Bartoschik T; Muyldermans S; Hoheisel JD The structural basis of nanobody unfolding reversibility and thermoresistance. *Scientific Reports*. 2018, 8, 7934. [PubMed: 29784954]
- (27). Li CL; Yang HJ; Yu WB; Yu XZ; Wen K; Shen JZ; Wang ZH Engineering of Organic Solvent-Tolerant Antibody to Sulfonamides by CDR Grafting for Analytical Purposes. *Analytical Chemistry*. 2021, 93, 6008–6012. [PubMed: 33728902]



**Figure 1.** (A) The positive clones identified by ic-ELISA through biopanning. (B) Sequence alignment of the selected Nbs, the framework regions (FRs) and complementary termination regions (CDRs) were determined by the IMGT database. (C) SDS-PAGE and western blotting analysis of purified Nb-7E.

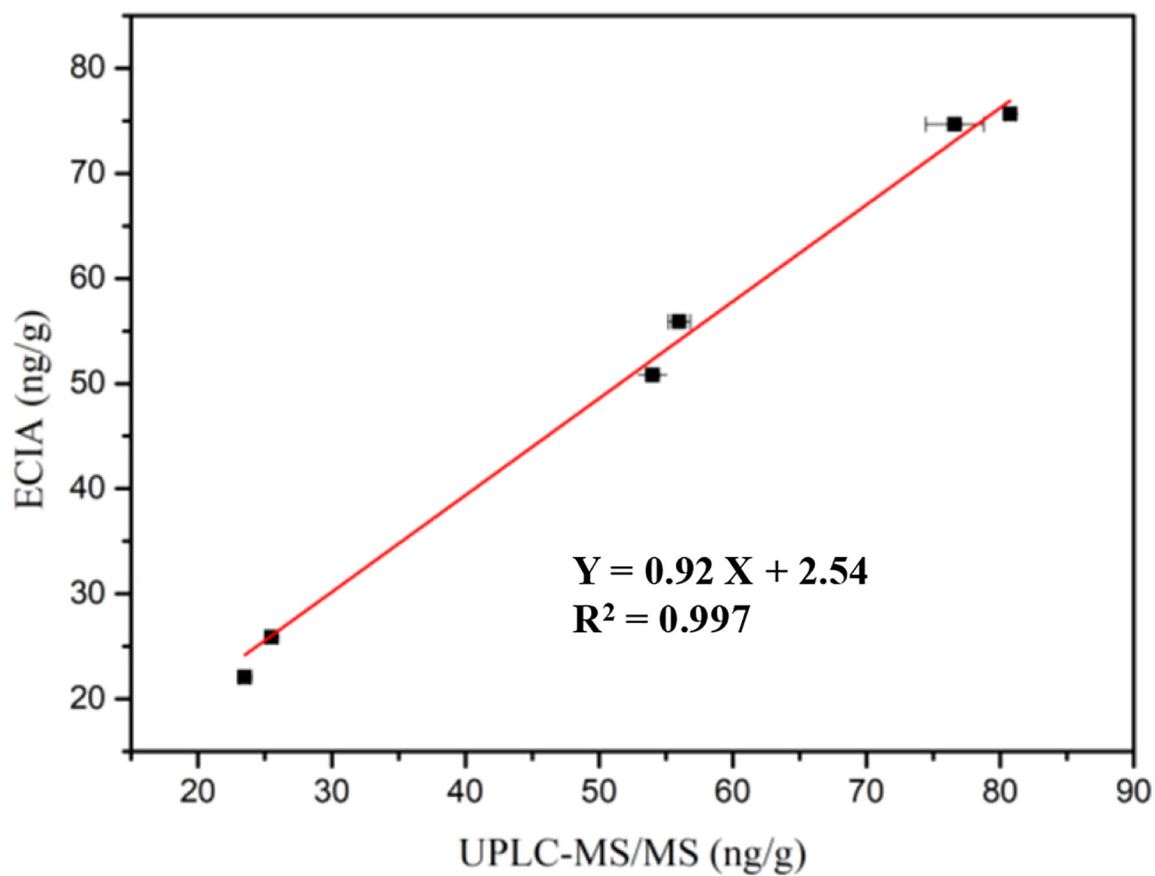
**Figure 2.**

(A) The retention of binding activity of Nb-7E for incubation at different temperatures for 5 min. (B) The thermostability of Nb-7E after being incubated at 85 °C for 10, 20, 30, 40, 50 and 60 min. Activity analysis of Nbs incubated with 10%–70% of methanol (C) and acetonitrile (D). (E) A standard curve of ic-ELISA based on Nb-7E. (F) Cross-reactivity determination of related analogs by ic-ELISA (n = 3).



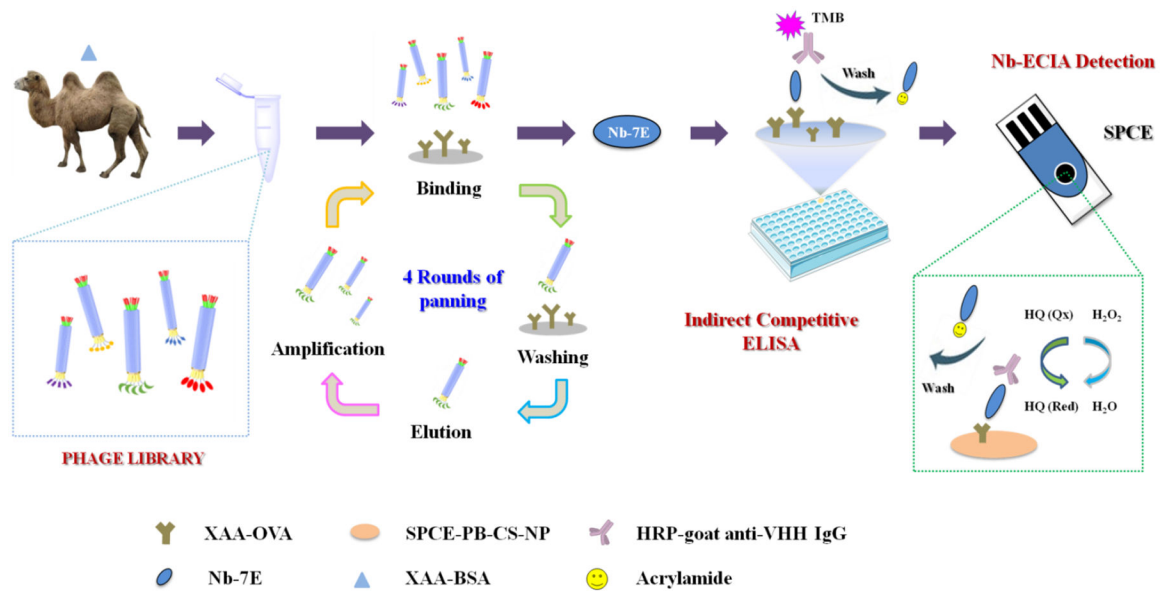
**Figure 3.**

Optimization and establishment of Nb-7E based ECIA. (A) XAA-OVA concentration, (B) Nb-7E dilution and (C)  $\text{H}_2\text{O}_2$  concentration. (D) Electrochemical current responses of Nb-based ECIA for the detection of different concentrations of AA: 0.39  $\mu\text{g/mL}$  (a), 0.78  $\mu\text{g/mL}$  (b), 1.56  $\mu\text{g/mL}$  (c), 3.125  $\mu\text{g/mL}$  (d), 12.5  $\mu\text{g/mL}$  (e), 25  $\mu\text{g/mL}$  (f), 50  $\mu\text{g/mL}$  (g). (E) Calibration curve of Nb-based ECIA between the different concentrations of AA and  $I$  values ( $n = 5$ ).



**Figure 4.** Correlations analysis between Nb-7E based ECIA and UPLC-MS/MS for AA in spiked samples.



**Scheme 1.**

Workflow of selection of nti-XAA Nb from an immunized Bactrian camel and development of ic-ELISA and ECIA based on anti-XAA Nb.

**Table 1**

Analytical characteristic of the ic-ELISA and ECIA based on Nb-7E for AA.

Parameters	ic-ELISA	ECIA
Coating antigen (ng)	200/well	50
Competition time (min)	30	30
Dilution of Nb-7E	1: 250	1: 40
LOD ( $\mu\text{g/mL}$ )	0.089	0.033
Linear range ( $\mu\text{g/mL}$ )	0.23–5.6	0.39–50
Assay time (min)	70	60

Author Manuscript

Author Manuscript

Author Manuscript

Author Manuscript

**Table 2**

Recovery analysis of AA in spiked samples by Nb-based ECIA (n = 3).

Samples	Background level (ng/g)	Spiked level (ng/g)	Found <sup>a</sup> ± SD <sup>b</sup> (ng/g)	Recovery <sup>c</sup> ± CV <sup>d</sup> (%)
Biscuits	289.50	25	22.07 ± 0.69	88.29 ± 3.13
		50	55.88 ± 1.11	111.76 ± 1.99
		75	75.66 ± 1.15	100.88 ± 1.52
Potato crisps	74.03	25	25.91 ± 0.11	103.64 ± 0.42
		50	50.79 ± 2.43	101.58 ± 4.78
		75	74.66 ± 3.48	99.55 ± 4.66

<sup>a</sup>Found value is calculated using measurement value to subtract background level<sup>b</sup>SD: standard deviation<sup>c</sup>Recovery = Found / Spiked level<sup>d</sup>CV: coefficient of variation = SD / Found